Analysis of Flux Fringing for High-Frequency AC Inductor Design

Anusyutha Krishnan, Parikshith B C, Vinod John
Department of Electrical Engineering
Indian Institute of Science
Bangalore, India 560012
Email:anusyutha@yahoo.co.in

***Abstract*—Design of high-frequency inductors for purposes like Active Front End (AFE) converter filters involves analytical calculations based on methods like area product approach and accurate graphical methods. Once a core with an area product is selected the subsequent calculations of inductance and peak operating flux requires the estimation of reluctance of the magnetic circuit. This in turn demands an estimate of the fringing that will happen in the air gap of the inductor. In this paper we have looked at analytical methods for evaluating fringing flux and compared it with results from finite element method. Different levels of details of modelling the inductor is first considered for this purpose. The end results are compared with experimental measurements of inductance. It is shown that simple fringing flux model can provide accurate models for the inductor design.**

Keywords: High frequency filter, Inductor, Finite Element Analysis, Fringing flux.

I. Introduction

Switching frequency filters are used in power converters to filter out ripple from the inverter output voltage. The inductors used for this in AC applications are rated for high power and are designed for high-frequency as well as the 50Hz fundamental frequency component of current. The design of these inductors are carried out by different methods, most of which require the determination of their magnetic reluctance.

The 'Area Product' equation is a good starting point for inductor design since it relates the electrical design inputs with material and geometric constraints. The traditional design steps using area product approach for inductor design first involves computing the area product [1]. This enables selection of the core. Now, for the selected core, number of turns of the inductor winding and air gap length have to be determined. The assumption is that the core reluctance is much lesser than the air gap reluctance and there is no fringing. As the permeability of core materials can vary significantly, the selection of a dominant air gap reluctance helps keep the inductance tolerance in an acceptable range.

A method that can be used for inductor design using the minimum number of turns for a given core selection is the graphical iterative approach [2]. It is based on the reasoning that in the design process of an inductor, there are two parameters that must be accurately preserved – the desired inductance, L, and the peak operating flux density in the core, B_m. And there are two parameters that can be adjusted – the number of turns, N, and the air gap length, l_g. So L and B_m are derived as functions of the two variables that can be adjusted.

Both these methods require the calculation of reluctance of the magnetic path in the inductor. This in turn depends on how accurately we can estimate the fringing in air gap. Fringing of flux is the phenomenon in which flux fringes or leaves the side of the core, thus shunting the air gap. Engineers designing power conversion magnetic components find the problem of fringing difficult to analyze and predict. Many times, the effect of fringing is being understood only after the design is done. Fringing flux creates a multitude of problems, especially while operating in high frequency range. It increases the area of cross-section of the air gap and the length of the magnetic path in the inductor. This causes a decrease in reluctance and introduces error in the estimation of its inductance value. As the air gap increases, the flux across the gap fringes more severely. Some of the fringing flux strikes the core and sets up eddy currents, which causes additional losses in the core. If the gap dimension gets too large, the fringing flux will strike the copper winding and produce eddy currents, generating heat, just like an induction heater. Hence an accurate estimation of fringing flux is critical in the design of inductors.

The proposed inductors were designed for the purpose of making LCL filters for grid-connected inverters. Area product approach and graphical iterative method were adopted for the design. The step-by-step procedure used for this design is discussed in [2]. The inductance of the manufactured inductors showed a considerable deviation from the initial designed value. Analysis using finite element method revealed that the fringing happening in the inductor air gap was the reason for this discrepancy.

The importance of taking into consideration fringing flux in the design of the inductors prompted us to look at the fringing effect in detail. We have come up with a method to estimate fringing by using Finite Element Analysis tools, which is explained in Section III of this paper. The following section briefly discusses the other methods used for the estimation of fringing in gapped inductors.

II. Analysis

The core used for the inductors was EE type as shown in Fig. 1. In the case of EE type core, there are three possible reluctances: Reluctance of the core $\Re_c$, reluctance of the center

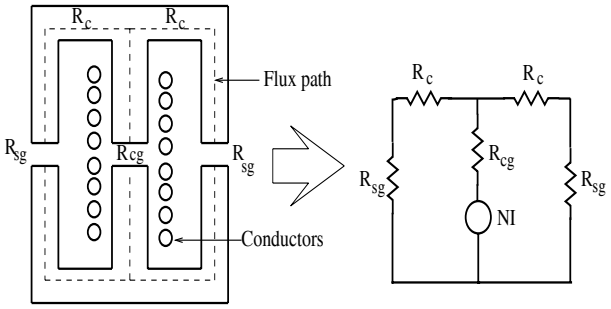

Fig. 1. Magnetic circuit representation of EE core inductor.

leg of E core $\Re_{cg}$ and reluctance of E core $\Re_{sg}$. The total reluctance of the magnetic path will be

$$\Re_t = \Re_{cg} + \frac{\Re_{sg}}{2} + \frac{\Re_c}{2}. \tag{1}$$

Inductance can be calculated from this by using the equation

$$L = \frac{N^2}{\Re_t}, \tag{2}$$

and the peak flux density can be expressed as

$$B_m = \frac{N I_p}{A_e \Re_t}, \tag{3}$$

where N is the number of turns of the inductor winding, I_p is the peak value of inductor current in amperes, A_e is the cross-sectional area of the core in m^2.

A. Simple Model

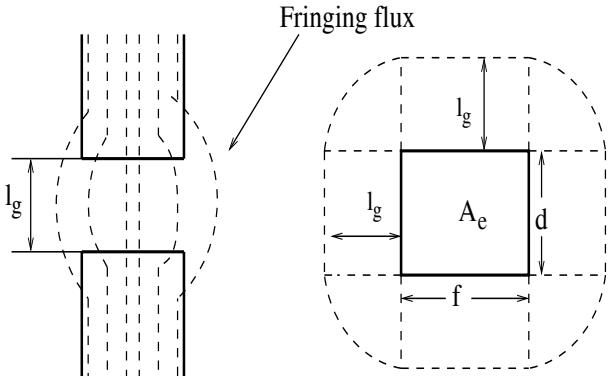

Fig. 2. Flux patterns for fringing effect analysis from [3].

The simple model proposed in this paper is a modification of the fringing estimate given by [3]. The fringing of the air gap is modelled as an increase in area of the air gap cross-section, and this increase is evaluated in terms of l_g. The initial assumption for air gap reluctance R_g for an air gap of l_g and core cross-section area $A_e = f \times d$ is given by

$$\Re_g = \frac{l_g}{\mu_0[A_e + (f+d)l_g + l_g^2]}. \tag{4}$$

The assumption of fringing in equation(4) made at the time of initial design could not accurately account for the actual fringing. The designed inductor was made of ferrite core with an air gap length of 12mm, which is a comparatively high value. At this value of air gap, the assumption that the flux fringes out to a distance of $l_g/2$ (where l_g is the air gap length), does not hold good. Equation(4) gave an error of 25% between calculated and measured inductance. The original equation was altered to reflect the actual inductance that was measured. The equation was modified to include fringing flux at the corners.

$$\Re_g = \frac{l_g}{\mu_0[A_e + 2(f+d)l_g + \pi l_g^2]} \tag{5}$$

This modification of the gap reluctance expression has been verified in section III based on the results of the finite element analysis.

B. Bossche and Valchev Model

The authors of [4] and [5] propose basic analytical approximations for fringing coefficients for several basic cases of air gap configurations. The total permeance of the air gap is a summation of the air gap permeance and product of these fringing coefficients multiplied by corresponding core dimensions. The permeances of each leg of EE core are calculated separately using the expressions for fringing coefficients.

$$\Lambda_g = \mu_0 \frac{a_e}{l_g} + \mu_0 C_g F \tag{6}$$

where Λ_g is the permeance of the air gap, a_e is the area of cross-section of the core, C_g is the core dimension (in m) corresponding to fringing coefficient F.

$$\Lambda_{cg} = \mu_0 \frac{2a_e}{l_g} + \mu_0[2(2f)F_2 + 2dF_1] \tag{7}$$

$$\Lambda_{sg} = \mu_0 \frac{a_e}{l_g} + \mu_0[3F_3 f + Cd] \tag{8}$$

$$\Lambda_c = \frac{\mu_i \mu_0 a_e}{l_g} \tag{9}$$

where Λ_{cg} is the permeance of air gap of center leg, Λ_{sg} is the permeance of the air gap of side leg,Λ_c is permeance of core. F_1, F_2 and F_3 are fringing coefficients. The corresponding reluctances are

$$\Re_{cg} = \frac{1}{\Lambda_{cg}} \; ; \; \Re_{sg} = \frac{1}{\Lambda_{sg}} \; ; \; \Re_c = \frac{1}{\Lambda_c}. \tag{10}$$

The net reluctance of the flux path is

$$\Re_t = \Re_{cg} + \frac{\Re_{sg}}{2} + \frac{\Re_c}{2}. \tag{11}$$

The parameters of the core and the inductor is listed in Table I [6]. The reluctance values for the designed inductor were calculated using the above two models and the comparison is given in Table II.

Core material	Ferrite (Epcos N87)
Core permeability	2200
Core type	UU 93/152/30 B67345
Number of turns	120
Current	14.58A
Inductance	3mH
Air gap length	12mm

TABLE I
SPECIFICATION OF INDUCTOR USED FOR FEA SIMULATION.

	Unit	Measured	Simple model	B & V model
$\Re_{cg}$	MH^{-1}		2.845	2.184
$\Re_{sg}$	MH^{-1}		3.557	2.574
L	mH	3.439	3.064	4.145
Error	%		-10.9	20.5

TABLE II
COMPARISON OF ACCURACY OF TWO FRINGING MODELS.

Simulation type	Inductance value (mH)
Single current sheet winding	1.89
Four layer winding	1.91
Individual conductors	1.99
3D simulation (four-layer winding)	2.35

TABLE III
INDUCTANCE VALUES FROM SIMULATION.

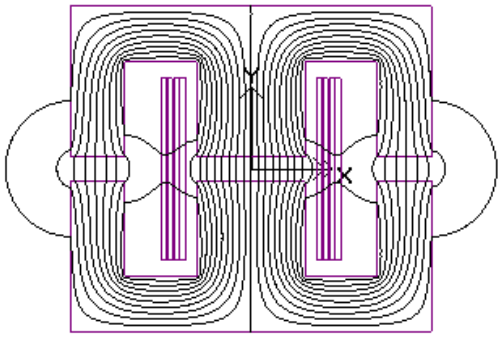

Fig. 3. Flux lines of the ferrite inductor from simulation

III. FINITE ELEMENT ANALYSIS

A. Simulation using FEA tools

The specifications of the inductor used for simulation are given in Table I. As a first approximation to the inductor geometry, the windings of the inductor were modelled as a single sheet of copper carrying current. A refined model with different layers of copper was chosen in the next step. Further refinement in the winding geometry was done by modelling the actual individual conductors in the winding. The inductance value can be calculated from the flux linkage or the energy. The core material has an initial permeability of 2200. Instead of using the non-linear BH curve specified in the manufacturer's data sheet, a linear model of the ferrite material was made use of. This was found to give results of reasonable accuracy. Size of the finite element mesh was varied and a mesh size of 3mm was found to be sufficient for 3D simulation,making a compromise between the accuracy and time for computation. Simulations were carried out using 2D as well as 3D time-harmonic solvers. The 3D simulation gave inductance values closer to the actual ones, but was found to be requiring more memory capacity and solving time. The simulations were done using the FEA tool MagNet [7]. Table III gives results from the simulation for inductance. Inductance was calculated from the FEA using flux linkage and energy methods. The size of the air box = 2 $\times$ maximum dimension of the inductor. The results of the FEA simulation studies are summarized in Table III.

B. Fringing calculation using FEA

To estimate how much the flux lines fringe out in the air gap of the inductor for various air gap lengths, the inductor was simulated by varying air gap length from 1mm to 24mm. Air gap flux density in the inductor was plotted for each case. Fig. 4 shows the plot of the air gap flux density versus distance across the air gap, at the centre line of the air gap. As expected, it can be seen that peak value of the flux decreases as one increases the air gap. Distances in Fig. 4 to Fig. 6 correspond to the X-direction in Fig. 3. This result is plotted for the side limb of the inductor. Fig. 5 shows the plot of normalised flux density. Normalisation was done by dividing each flux density value by the maximum value of flux density in the air gap. Maximum value of flux density occurs at the center of the air gap. Flux in the air gap was calculated by integrating the flux density value over the air gap area. To capture 100% of the flux in the air gap, one needs to go to the extend of the airbox used in the FEA simulation, as can be observed from the figure. It was seen that the distance for capturing 80-90% of the flux was a sufficient engineering approximation for obtaining a sufficiently accurate air gap reluctance. Trapezoidal rule of integration was employed for the evaluation of flux from the flux density. Fringing distance was taken as the distance at which the flux falls to 85% of maximum flux which is normalized to one at the outer boundary and zero at the middle of the gap. It can be seen from Fig. 5 that the flux extends further out into the air towards the left side of the figure. This is because the winding which is placed to the right side of the limb in the figure, shields the flux better than air, which is on the left side. For the following analysis, fringing distance is considered as the distance that one needs to go beyond the edge of the core so that 80-90% of the net flux is included in that area. Fringing factor, k_f, is the ratio of fringing distance to air gap length.

Fig. 7 shows the plot of fringing distance, D_f, against air gap length. The two straight lines in Fig. 7 correspond

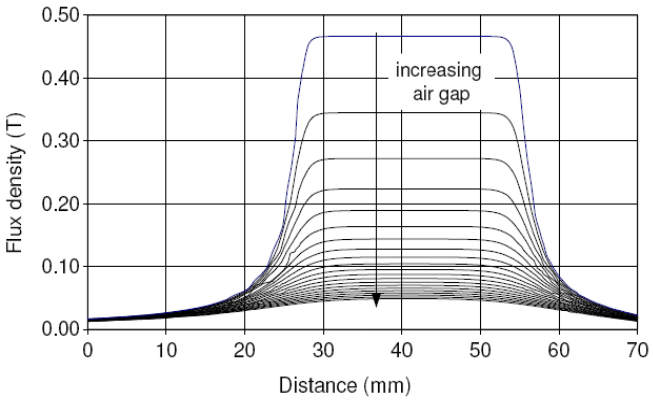

Fig. 4. Flux density as a function of distance along side limb of the E core along the center line of the air gap. The air gap distance is varied from 3mm to 24mm in steps of 1mm.

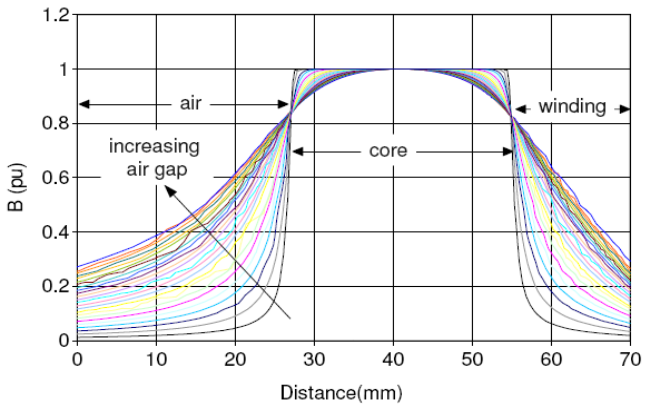

Fig. 5. Plot of normalised flux density versus distance along airgap for the sidelimb of the core. The curves are for airgap varying from 3mm to 24mm in steps of 1mm.

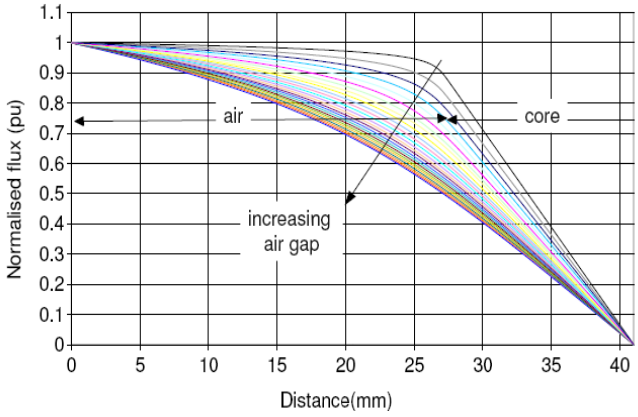

Fig. 6. Plot of normalised flux versus distance along airgap for the sidelimb of the core. The curves are for airgap varying from 3mm to 24mm in steps of 1mm.

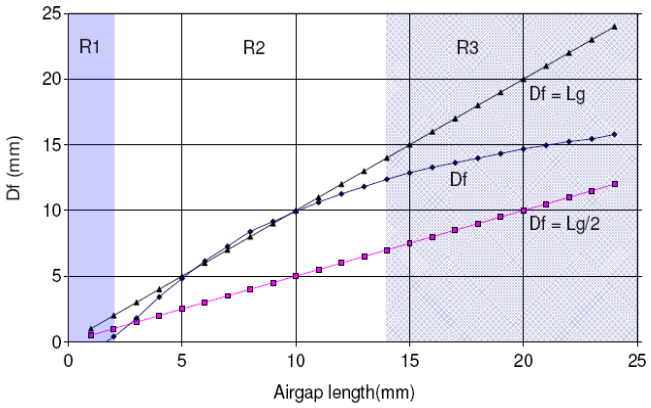

Fig. 7. Fringing distance (D_f) for different airgaps for the sidelimb of the EE core. Region R1 corresponds to very small airgap, R2 for typical airgaps and R3 for large airgaps.

to fringing distances of $l_g/2$ and l_g, corresponding to the approximations in equations (4) and (5). D_f takes values very close to $l_g/2$ at the lower range of air gap lengths. D_f increases with increase in air gap, and from the plot it is found that for an air gap length of 12mm, which is our design value, the fringing edge is almost equal to the air gap length l_g and not $l_g/2$ as assumed initially. Region $R1$ in Fig. 7 corresponds to having a small air gap where the tolerances of the core properties can be significant. Region $R3$ corresponds to having a very large air gap that is larger than the core width. In this case transverse flux lines can become a significant consideration for the design. Region $R2$ is a suitable air gap range for the design of the inductor.

Fig. 8 shows that the fringing factor k_f can be taken as 0.5 for small air gap designs and as 1.0 for large air gap designs. However, using an actual fringing flux factor based on the selected airgap length can lead to more accurate design. Table II shows a comparison between the designed and measured inductance values. The simple model of fringing and fringing approximation using Finite Element Analysis are found to give values of inductance closer to the actual inductance value to within 10% of the measurement.

IV. Conclusion

The results of analysis done using FEA matches with that of the simple fringing model. This paper studied two analytical methods of capturing fringing flux for inductor design. Based on the results of finite element analysis, a modified simple model of fringing was found suitable for large air gap inductor designs. The final inductance was within 10% of the measured inductance. The FEA study indicates that a single multiplier for the fringing distance may not be sufficient for all situations. The analytical expression for reluctance including fringing effects can lead to sufficiently accurate design without requiring extensive FEA studies.

Acknowledgement

The authors would like to thank National Mission for Power Electronics Technology (NaMPET), a national mission program under Ministry of Communications and Information Technology, Government of India for funding this project.

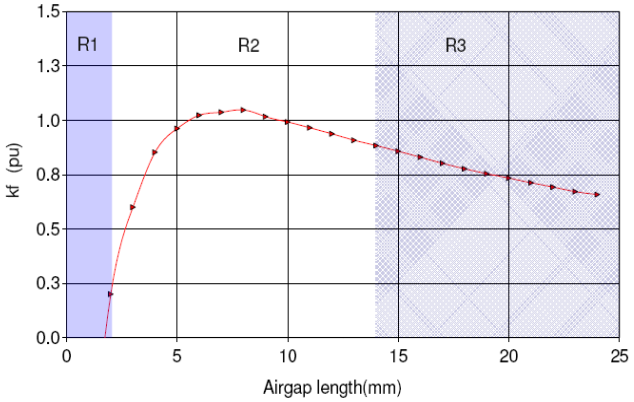

Fig. 8. Fringing factor (k_f) for different airgaps for the sidelimb of the EE core. Region R1 corresponds to very small airgap, R2 for typical airgaps and R3 for large airgaps.

REFERENCES

[1] Col. Wm. T. McLyman, "Magnetic cores", in *Transformer and Inductor Design Handbook*, 3rd ed., Marcel Dekker, 2004, pp. 3-1–3-48.

[2] Parikshith B C, Vinod John, *"Higher Order Output Filter Design for Grid Connected Power Converters,"* Fifteenth National Power Systems Conference (NPSC), IIT Bombay, December 2008.

[3] G.S. Ramana Murthy, *Design of Transformers and Inductors at Power-Frequency A modified Area-Product method*, M.Sc(Engineering)Thesis, Indian Institute of Science, March 1999.

[4] A. Van den Bossche, V. Valchev, T. Filchev, *"Improved approximation for fringing permeances in gapped inductors,"* Industry Applications Conference, 2002. 37th IAS Annual Meeting Conference Record of the, 2002, vol.2, pp. 932-938.

[5] A. Van den Bossche, V. Valchev, *Inductors and Transformers for Power Electronics,* 1st ed., Taylor and Francis, 2005, pp. 333-342.

[6] *Ferrites and Accessories Catalog: EPCOS, (2007).* `http://www.epcos.com`

[7] *Infolytica Corporation, MagNet User guide.* `http://www.infolytica.com`

Anusyutha Krishnan received her BTech (Electrical and Electronics Engineering) degree from NIT, Calicut, India. Subsequently, she worked for over a year and half as a Project Assistant in Power Electronics Group in the Department of Electrical Engineering at the Indian Institute of Science, Bangalore, India.

Her research interests include renewable energy technology and power electronics. Outside engineering stream, interested in working among children for training them in life skills.

Parikshith B.C received B.E degree in Electrical and Electronic Engineering from Visvesvaraya Technological University, Belgaum, India in 2006 and M.Sc (Engineering) degree in Electrical Engineering from Indian Institute of Science, Bangalore, India in 2010.

His research interests include renewable energy, distributed generation, magnetic components and power quality.

Vinod John received B.Tech. degree in Electrical Engineering from the Indian Institute of Technology, Madras, M.S.E.E. degree from the University of Minnesota, Minneapolis, and Ph.D. from the University of Wisconsin, Madison. He has worked in research and development positions at GE Global Research, Niskayuna, NY and Northern Power, VT. He is currently working as an Assistant Professor at the Indian Institute of Science, Bangalore.

His primary areas of interests are in power electronics and distributed generation, power quality, high power converters and motor drives.